Res. Commun. 163, 424-429.
Ni, F., Scheraga, H. A., & Lord, S. T. (1988) *Biochemistry 27*, 4481-4491.
Nilges, M., Clore, G. M., & Gronenborn, A. M. (1988) *FEBS Lett. 229*, 317-324.
Nilges, M., Clore, G. M., & Gronenborn, A. M. (1990) *Biopolymers 29*, 813-822.
Olejniczak, E. T., Gampe, R. T., Jr., & Fesik, S. W. (1986) *J. Magn. Reson. 78*, 28-41.
Otting, G., Widmer, H., Wagner, G., & Wüthrich, K. (1986) *J. Magn. Reson. 66*, 187-193.
Pease, J. H., & Wemmer, D. E. (1988) *Biochemistry 27*, 8491-8498.
Pelton, J. T. (1991) *Neurochem. Int. 18*, 485-489.
Perkins, T. D. T., Hider, R. C., & Barlow, D. J. (1990) *Int. J. Pept. Protein Res. 36*, 128-133.
Price, W. S., Medz, G. L., & Martenson, T. E. (1988) *Biochemistry 27*, 8990-8999.
Reily, M. D., & Dunbar, J. B., Jr. (1991) *Biochem. Biophys. Res. Commun. 178*, 570-577.
Rose, G. D., Gierasch, L. M., & Smith, J. A. (1985) *Adv. Protein Chem. 37*, 1-106.
Saudek, V., Hoflack, J., & Pelton, J. T. (1989) *FEBS Lett. 257*, 145-148.
Saudek, V., Hoflack, J., & Pelton, J. T. (1991) *Int. J. Pept. Protein Res. 37*, 174-179.
States, D. J., Haberkorn, R. A., & Ruben, D. J. (1982) *J. Magn. Reson. 48*, 286-292.
Tamaoki, H., Kobayashi, Y., Nishimura, S., Ohkubo, T., Kyogoku, Y., Nakajima, K., Kumagaye, S., Kimura, T., & Sakakibara, S. (1991) *Protein Eng. 4*, 509-518.
Summers, M. F., South, T. L., Kim, B., & Hare, D. R. (1990) *Biochemistry 29*, 329-340.
Wüthrich, K. (1986) *NMR of Proteins and Nucleic Acids*, Wiley, New York.
Wüthrich, K., Billeter, M., & Braun, W. (1983) *J. Mol. Biol. 169*, 949-961.
Yanagisawa, M., & Masaki, T. (1989) *Trends Pharmacol. Sci. 10*, 374-378.
Yanagisawa, M., Kurihara, H., Kimura, S., Tomobe, Y., Kobayashi, M., Mitsui, Y., Yazaki, Y., Goto, K., & Makaki, T. (1988) *Nature 332*, 411-415.
Zuiderweg, E. R. P., Boelens, R., & Kaptein, R. (1985) *Biopolymers 24*, 601-611.

Spectroscopic Evidence for an Intermediate in the T_6 to R_6 Allosteric Transition of the Co(II)-Substituted Insulin Hexamer†

Larry Gross‡ and Michael F. Dunn*
Department of Biochemistry, University of California at Riverside, Riverside, California 92521-0129
Received August 5, 1991; Revised Manuscript Received October 31, 1991

ABSTRACT: The phenol-induced conformational transition in the insulin hexamer is known to involve a large change in structure wherein residues 1-8 of the insulin B-chain are transformed from an extended coil (T-state) to a helix (R-state). This change in protein conformation both exposes a cryptic protein pocket on each subunit to which phenol binds and forces the HisB10 zinc sites to undergo a change in coordination geometry from octahedral to tetrahedral [Derewenda, U., Derewenda, Z., Dodson, E. J., Dodson, G. G., Reynolds, C. D., Smith, G. D., Sparks, C., & Swensen, D. (1989) *Nature 338*, 593-596]. Substitution of Co(II) for Zn(II) at the HisB10 sites introduces a sensitive chromophoric probe of the structural and chemical events that occur during this allosteric transition [Roy, M., Brader, M. L., Lee, R. W.-K., Kaarsholm, N. C., Hansen, J. F., & Dunn, M. F. (1989) *J. Biol. Chem. 264*, 19081-19085]. In this study, using rapid-scanning stopped-flow (RSSF) UV-visible spectroscopic studies, we demonstrate that a transient chemical intermediate is formed during the phenol-induced conversion of Co(II)-substituted hexamer from the T-state to the R-state. Decomposition of the RSSF spectra gave a spectrum for the intermediate with *d-d* transitions consistent with the assignment of the intermediate as either a distorted tetrahedral or a 5-coordinate Co(II) species. Possible structures for the intermediate and the implications of these findings to the allosteric mechanism are considered.

Crystallographic structure determinations (Baker et al., 1988; Derewenda et al., 1989) have shown that the T_6 to R_6 conformational change involves large alterations both of the conformation of residues 1-8 of the insulin B-chain and of the geometry of the HisB10 metal sites.[1] The conformation of residues B1-B8 is extended in the T-state and coiled to a helix in the R-state. The T_6-R_6 transition is driven by ligand binding; the change to a helical conformation opens six binding pockets for phenol which are occluded in the T-state by the LeuB6 side chains. The HisB10 metal sites undergo a change in geometry from octahedral coordination in the T-state (with a ligand field consisting of three HisB10 imidazolyl moieties and three water molecules), to tetrahedral coordination in the R-state (wherein the three water molecules are replaced by

† Supported by NIH Grant 1-RO1-DK 42124-02.
* To whom correspondence should be addressed: Department of Biochemistry 015, University of California at Riverside, Riverside, CA 92521-0129.
‡ Present address: Upjohn Co., Kalamazoo, MI 49001.

[1] Abbreviations: T, the conformation of an insulin subunit in the two-zinc hexamer; R, the conformation of an insulin subunit in the phenol-induced hexamer; T_6, T_3R_3, and R_6, the three crystallographically identified allosteric forms of the insulin hexamer; M(II)-T_6 or M(II)-R_6 (where M = Zn or Co), the metal ion substituted in the HisB10 sites of the insulin hexamer; RSSF; rapid-scanning stopped flow; SWSF, single-wavelength stopped flow.

0006-2960/92/0431-1295$03.00/0

a single anionic ligand). Consequently, the conformational transition is an allosteric process (Kaarsholm et al., 1989), and the work of Brader et al. (1991) and Brader and Dunn (1990) has established that heterotropic interactions between the phenol pockets and the HisB10 metal sites and homotropic interactions among the phenol pockets strongly influence the thermodynamics of the transition.[2]

When Co(II) is substituted for Zn(II) at the HisB10 sites, the resulting insulin–cobalt complex, Co(II)–T_6, is isomorphous to the native Zn(II)–T_6 hexamer. Previous work from this laboratory (Roy et al., 1989; Brader et al., 1990; Brader & Dunn, 1990; Brader et al., 1991) has established that Co(II)–T_6 undergoes the conformational change to Co(II)–R_6 upon reaction with an excess of phenol. In the T_6 state, the Co(II) centers exhibit the small molar extinction coefficients typical of octahedral coordination ($\epsilon \simeq 90$ M^{-1} cm^{-1} at 490 nm). The R_6 state of the Co(II) hexamer is characterized by the relatively strong, visible absorbance bands typical of tetrahedral coordination ($\epsilon \simeq 500$ M^{-1} cm^{-1} at 530–620 nm). Therefore, a strong spectroscopic signal marks the T_6–R_6 transition of the Co(II)-substituted insulin hexamer.

Using rapid-scanning, stopped-flow (RSSF) UV–visible spectroscopy and the chromophoric signals derived from the *d–d* transitions of the Co(II)-substituted hexamer, we have carried out a preliminary investigation of the mechanism of the T to R allosteric transition. Central to this paper is the spectroscopic evidence for an intermediate formed during the phenol-induced conversion of T_6 to R_6. As will be shown herein, when a solution of phenol is rapidly mixed with Co(II)–T_6 in a stopped-flow observation cuvette and monitored via UV–visible RSSF spectroscopy, the family of time-resolved spectra establish that the transition of Co(II)–T_6 to Co(II)–R_6 occurs via the formation and decay of a chromophoric intermediate with a unique envelope of *d–d* transitions. The formation of the intermediate is likely related to the conformational transition of the protein, and decay of this species appears to be controlled by ligand substitution processes. Experiments are presented which explore both the mechanism of intermediate formation and possible structures for the intermediate.

Materials and Methods

Human and porcine insulin were gifts supplied by Novo-Nordisk (Bagsvaerd, Denmark) as metal-free lyophilized powders. The insulin–cobalt complex was prepared by dissolving this powder in buffer, which was 100 mM tris(hydroxymethyl)aminomethane (Tris; Sigma Chemical, St. Louis, MO), and the pH was adjusted to 8.0 by adding perchloric acid. The concentration of the dissolved insulin was determined spectrophotometrically, using the 280-nm band (ϵ = 5700 M^{-1} cm^{-1}; Porter, 1953). A stoichiometric amount of cobalt (in the ratio 2 g-atom/hexamer) was then added, using a 100 mM stock solution of cobalt(II) perchlorate (Alfa, Danvers, MA) in H_2O. When NaCl or KSCN was present, these salts were added to the buffer prior to the addition of insulin or Co(II). NaCl and KSCN were supplied by Mallinckrodt (St. Louis, MO).

Phenol (J. T. Baker, Phillipsburg, NJ) was dissolved in buffer at an initial concentration of 200 mM. Upon mixing with Co(II)–T_6 in the RSSF apparatus, the phenol concentration was reduced by half, to 100 mM. In the Results section, the concentrations of each reactant after mixing are specified. Added ions, like Cl^-, I^-, and SCN^-, were of equal concentration in both solutions, and so these were not reduced by dilution in the stopped-flow instrument.

The RSSF apparatus consists of a modified Durrum D110 stopped-flow instrument custom-fitted with an optical multichannel analyzer, EG&G Princeton Applied Research Model 1460. Details of the RSSF system and operating procedures have been published elsewhere (Koerber et al., 1983). Five hundred pixels of the Si diode detector array were scanned to obtain visible absorbance spectra in the 450–700-nm region using a repetitive scanning time of 8.544 ms/scan. A subset of 25 spectra was stored from each stopped-flow reaction run. Ignored scans were interspersed to adjust the length of time between stored scans along the reaction time course. Thus, the total reaction time in Figure 1 was 1.7 s. The RSSF spectra reported in Figures 1–3 were collected with the following timing sequence: (1) 8.53, (2) 17.1, (3) 25.6, (4) 34.1, (5) 42.7, (6) 59.7, (7) 76.8, (8) 93.8, (9) 110.1, (10) 128.0, (11) 179.1, (12) 230.3, (13) 281.5, (14) 332.7, (15) 383.9, (16) 477.7, (17) 571.5, (18) 655.3, (19) 759.2, (20) 853.0, (21) 1023.6, (22) 1194.2, (23) 1364.8, (24) 1535.4, and (25) 1706.0 ms.

In single-wavelength stopped-flow (SWSF) kinetic studies, reactants are likewise rapidly mixed in an observation cuvette with a separate Durrum apparatus. A single wavelength is selected by a monochromator to monitor the reaction, and data are acquired using a desktop computer interfaced to the photomultiplier detector. The absorbance–ordinate time courses were fit by nonlinear least-squares regression, using the program KINFIT (On-line Instrument Systems, Inc., Jefferson, MO).

Results

Parts A and B of Figure 1 show the RSSF spectra obtained when Co(II)–T_6 reacts with phenol in either the absence (A) or presence (B) of 100 mM Cl^-. The convergence of the traces with increasing absorbance indicates that the reaction had run its course. In the last few traces, the spectrum of Co(II)–R_6 predominates. For clarity, not all 25 traces of the instrument buffer memory are displayed in Figure 1A,B. In these RSSF studies, the experiment dead-time consists of the mixing and the scan acquisition dead time (typically 12–15 ms in duration).

In most of these experiments, the stoichiometry of cobalt(II) ions to insulin hexamer is 2:1. Any error in this ratio due to pipetting was likely to be small. However, to ensure that there was no effect on the results from errors due to deviation from a 2:1 stoichiometry, SWSF kinetic measurements were compared with cobalt:hexamer ratios of 1, 1.5, 1.8, 2.0, and 2.2. When Co(II)–T_6 with a ratio less than 2 was mixed with phenol, the amplitude of the absorbance change was reduced correspondingly. With excess cobalt, no increase in signal was observed. In both cases, the relaxation rate constants retrieved were within 5% of the value obtained for a 2:1 stoichiometry. These results indicate that extraneous reactions of insulin or cobalt do not significantly perturb the time courses for the conformation change.

In the presence of phenol, very different spectral changes resulted depending on what anions were present in solution (viz., parts A and B of Figure 1). The tetrahedral cobalt coordination sphere in Co(II)–R_6 consists of three B10 histidines from each of three insulin subunits. The fourth coordination position is occupied by a ligand from solution. The

[2] Equilibrium titrations of the visible spectral changes which accompany the phenol-mediated conversion of Co(II)–T_6 to Co(II)–R_6 yield sigmoidal absorbance vs [phenol] isotherms with an apparent Hill coefficient $n_H \simeq 2$, and anionic ligands are positive effectors of this apparent positive cooperativity (E. Choi, V. Aguilar, M. L. Brader, N. C. Kaarsholm, and M. F. Dunn, manuscript in preparation).

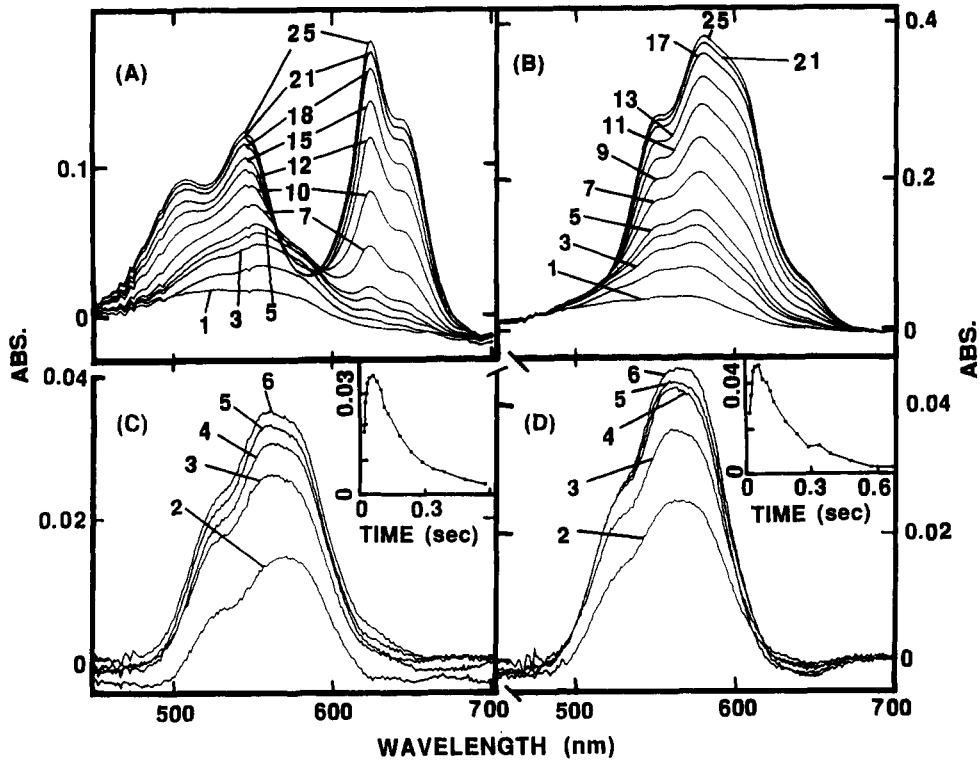

FIGURE 1: The spectroscopic time courses for the reaction of 0.17 mM Co(II)–T_6 with 100 mM phenol at pH 8.0 in the absence (A, C) and presence (B, D) of 100 mM chloride ion. (A) Reaction in the absence of chloride ion. The time interval between scans is 8.54 ms for the first five spectra, followed by spectra at successively longer intervals afterward (see Materials and Methods). The total acquisition time was 1.71 s for the 25 spectra collected; only spectra numbers 1–5, 7, 10, 12, 15, 18, 21, and 25 are shown. (B) Reaction in the presence of 100 mM chloride ion. The timing sequence of the spectra is the same as that of part A. For clarity, spectra 6, 8, 10, 12, 14–16, 18–20, and 22–24 have been omitted. (C) The scaled, subtracted spectra calculated from the second to the sixth spectrum of part A, corresponding to the time course for intermediate formation. The time course plotted in the inset shows the absorbance change at 560 nm for the complete set of scaled, subtracted spectra as a function of time. (D) Scaled, subtraction spectra numbers 2–6, as in part C, for the data part B, with chloride ion present. The inset plot also shows the time course at 560 nm obtained from the complete set.

effects of ligand structure on the Co(II)–R_6 spectrum have been characterized for a wide variety of anionic and neutral ligands coordinated to the fourth ligand position (Roy et al., 1989; Brader et al., 1990, 1991). In Figure 1A, where the anions present are restricted to ClO_4^-, OH^-, and phenoxide ion, the fourth ligand has been determined to be phenoxide (Brader et al., 1991). When chloride ion was present, as in Figure 1B, the fourth ligand has been shown to be Cl^- (Roy et al., 1989; Brader et al., 1990, 1991).

Close inspection of Figure 1A in the wavelength region between 570 and 590 nm revals the appearance of a species spectroscopically distinct from the final R-state of the cobalt–insulin hexamer. This species reaches maximum absorbance on the sixth scan, collected ca. 60 ms after flow stops.

In Figure 1B, a single large band developed at 580 nm for Co(II)–R_6 with Cl^- present. Although the formation and decay of an intermediate species such as in Figure 1A is not obvious from inspection of these RSSF spectra, SWSF kinetic studies (data not shown) indicated that the time course consists of at least three relaxations.

To extract the spectra of the intermediates formed in Figure 1A,B from the spectra of reactants and final products, scaled subtractions were calculated for each data set. The results are shown in parts C (absence of Cl^-) and D (presence of 100 mM Cl^-) of Figure 1. These scaled subtractions were computed in the following way: To compensate for variations in the baseline, the first scan was subtracted from each subsequent scan. The last spectrum of the set (the 25th scan saved to memory minus the first) was then multiplied by a scale factor. The factor was calculated by dividing the absorbance of a spectrum at time t into that of the final spectrum at a wavelength (624 nm) away from that of the transient band. At this wavelength, the transient band makes negligible contributions to the spectra. This factor represents the fraction of the final Co(II)–R_6 absorbance contributing to each spectrum collected during the time course of the reaction and, therefore, corresponds to the fraction of Co(II) in the form of final product. This factor increased for each scaled subtraction, typically from 0.03 for the second scan to 0.9 for the later scans. Thus, the last scan minus the first scan, multiplied by this factor, results in a spectrum approximating a Co(II)–R_6 spectrum for the instant in the time course at which the factor was calculated. The scaled Co(II)–R_6 spectrum was then subtracted from the corresponding spectrum in the set to give the scaled subtraction spectra. The resulting subtracted spectra, shown in parts C and D of Figure 1, represent the progress of the reaction during intermediate formation with the absorbance contributions of the starting material and final product removed.

Because the spectrum of the intermediate (Figure 1C) is similar in band shape and excitation energy to the spectrum of the Co(II)–R_6–Cl^- complex (spectrum 25 of Figure 1B), experiments were carried out (data not shown) to determine if the intermediate is simply a minor species resulting from chloride ion contamination. The transient absorbance at 570 nm in Figure 1A did not depend on the presence or absence of low concentrations of chloride ion. Despite the dissimilarity in the final Co(II)–R_6 spectra obtained with or without Cl^-, the spectral profile and time-resolved appearance and decay of the transient remained unchanged.

From comparison of parts C and D of Figure 1, it appears that the spectral profile obtained for the intermediate is es-

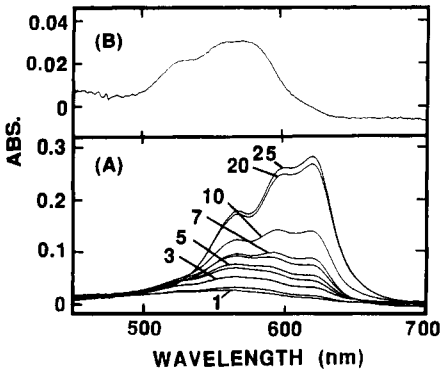

FIGURE 2: (A) The sequence of RSSF spectra for the reaction of 0.17 mM Co(II)–T_6 insulin with 100 mM phenol in the presence of 50 mM sodium iodide, pH 8.0. For clarity, the first seven spectra collected at intervals of 8.54 ms are shown followed by spectra 10, 20 and 25. The total acquisition time was 1.71 s. (B) The scaled, subtracted spectrum for spectrum number 6 of the RSSF sequence collected ~51.2 ms after mixing.

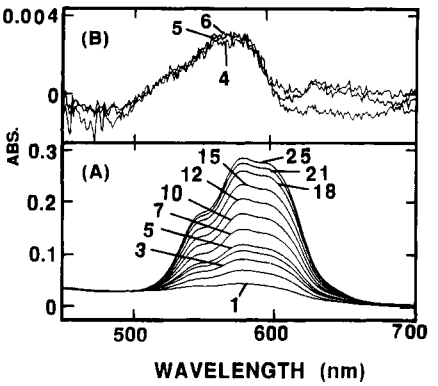

FIGURE 3: (A) The RSSF spectra for the reaction of 0.17 mM Co(II)–T_6 with 100 mM phenol, pH 8.0, in the presence of 5 mM thiocyanate ion. The timing sequence is the same as in Figure 1A, and the scaled subtraction spectra shown in (B) (spectra numbers 4, 5, and 6) were extracted from the RSSF data set as described in Figures 1 and 2.

sentially the same whether or not a high concentration of Cl^- was present. To simplify the comparison, the scaled subtractions are shown only for spectra numbered 2–6 of the original data sets. The slight differences in the baseline between parts C and D were attributed to differences in the mixing dead time of the RSSF instrument before data collection was initiated. The slight differences in the shape of the peak between 560 and 570 nm were likewise due to the degree of advancement of the reaction before the first scan is measured.

The peak absorbance in Figure 1C,D at 560 nm began to decay after the sixth scan. The later subtracted spectra were also plotted, and the baseline-corrected absorbance at 560 nm was measured. The resulting amplitudes were plotted against the time of the scan to give the time courses shown in the insets of Figure 1C,D. The rate of appearance and decay of the transient was found to be very similar for the two experiments.

The result implied by these experiments is one of two alternatives. The kinetic time courses (Figure 1) demonstrate that the rates of intermediate formation and decay satisfy the criterion of kinetic competence [see Bunnett (1974)]. Therefore, either Co(II)–T_6 reacts to form an intermediate along the reaction pathway for the T to R conformational transition or the species represented by the transient spectrum is simply a side reaction unrelated to the final outcome (i.e., a cul-de-sac).

The RSSF spectra presented in Figure 2 show that the Co(II)–R_6–iodide system gives a final spectrum with an envelope of peaks located in the 600–618-nm region that is quite different from that of the complexes with phenoxide ion or chloride ion. The appearance of an intermediate in the iodide system with a spectrum essentially identical to that of the intermediates formed when the final R-state complexes contain either phenoxide ion or chloride ion coordinated to Co(II) is evident (compare parts C and D of Figure 1 with Figure 2B). These data provide further evidence indicating that the species responsible for the transient bands seen in Figure 1C,D appears regardless of whether the anion which becomes incorporated into the fourth ligand position is phenoxide ion, chloride ion, or iodide ion (viz., Figures 1 and 2).

When Co(II)–T_6 reacts with phenol to form Co(II)–R_6 in the presence of thiocyanate ion, the tetrahedral cobalt center coordinated to SCN^- gives a spectrum very similar to the R-state spectrum obtained when Cl^- is present. The λ_{max} of the Co(II)–R_6–SCN^- complex occurs 5 nm red-shifted from that of the Co(II)–R_6–Cl^- complex. The RSSF experiment comparable to Figure 1 but carried out with 5 mM SCN^- in place of Cl^- is shown in Figure 3. The results of scaled substractions calculated in a fashion analogous to those in Figure 1C,D, are shown in Figure 3B. It is obvious that in spite of the similarities between the spectra of the Co(II)–R_6 complexes of Cl^- and SCN^-, the transient peak at 560 nm is much weaker (near the limits of detection) when SCN^- is present.

Much higher thiocyanate ion concentrations (≥0.4 mM) cause conversion of Co(II)–R_6 to a mixture of octahedrally and tetrahedrally coordinated cobalt, when no phenol is present (Brader et al., 1991). When the RSSF experiment of mixing Co(II)–T_6 with 100 mM SCN^- (final concentration) was carried out, each spectrum in the set was found to be similar to the final spectrum (Figure 3), and no transient peak at 560 nm was detected in subtracted spectra. When the reaction was carried out in the presence of 50 mM NaN_3 and 100 mM phenol (data not shown), no transient intermediate was detected.

Further RSSF experiments were conducted to help elucidate the structure of the species giving the transient absorbance at 560 nm. Possible contamination of the sample by ions other than chloride ion which might be a source of the band was investigated. For example, acetate ion is known to coprecipitate with insulin in the manufacturing process, and both acetate ion and nitrate ion (in high concentrations) give complexes with Co(II)–R_6 that display *d–d* transitions in the 500–600-nm region (Brader et al., 1990, 1991). However, neither the addition of acetate nor that of nitrate ions at concentrations in the 1–10 mM range gave any difference in either the kinetics of intermediate formation and decay or the band shape or amplitude. Under these conditions, the final product is the phenoxide ion complex. Variation in the pH of the Tris buffer from pH 7 to 9 also did not have any significant effect. These results indicate that the species responsible for the peak at 560 nm is not due to a side reaction involving acetate or nitrate ion contaminants.

RSSF experiments were performed with varying concentrations of phenol; the absorbance maximum of the intermediate, after subtraction, was found to be proportional to the phenol concentration. This result was obtained whether or not chloride ion was present. The finding that the amount of intermediate produced depends significantly on the concentration of phenol and that the intermediate appears not to be a consequence of a side reaction with contaminating anions (e.g., Cl^-, NO_3^-, or acetate ion) indicates that the intermediate

Scheme I: Mechanism Proposed for the Phenol-Mediated Interconversion of the Co(II)-Substituted T- and R-State Insulin Hexamers[a]

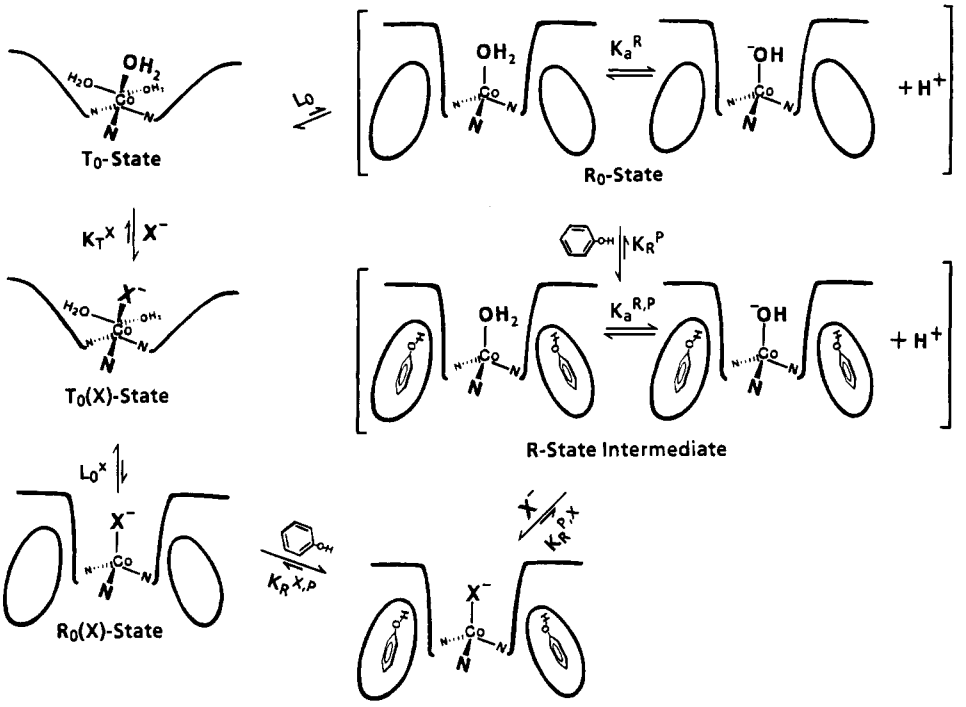

[a] In each cartoon, a portion of each hexamer has been cut away to reveal the metal ion geometry, the coordinating ligands, and the protein conformation about one HisB10 site. T-state HisB10 sites are shown located in shallow depressions near the surface of the hexamer. R-state HisB10 sites are positioned at the bottom of narrow tunnels that run along the 3-fold symmetry axis. The protein pockets of the R-state that bind phenol are shown as ovals. These sites are covered and are therefore believed to be incapable of binding phenol in the T-state. In the absence of phenol or other allosteric effectors, the allosteric constant $L_0 = [T_0]/[R_0] > 1$. When the ligand X^- = phenoxide ion, iodide ion, or azide ion, then $L_0^X = [T_0(X)]/R_0(X)] > 1$, whereas when X^- = thiocyanate ion, $L_0^X < 1$. The intermediate detected in the kinetic studies shown in Figures 1 and 2 is depicted here as either the R-state water or hydroxide ion complex.

is an obligatory chemical species in the mechanism of the T to R transition.

Discussion

Because the time courses for the T to R transition consist of at least two phases and the individual relaxations show an interesting, but complicated, dependence on the concentration of phenol, the work presented herein is focused on the spectroscopic characterization of the intermediate. A more detailed and quantitative analysis of the system is now in progress.

The increase in absorbance which constitutes the overall signal change in these experiments is dependent upon the formation of a tetrahedral configuration at the Co(II) center (Roy et al., 1989; Brader et al., 1990, 1991). The shape of the *d–d* envelope and the intensity of this band indicates that the intermediate is either a distorted tetrahedral complex or a pentacoordinate complex (Cotton & Wilkinson, 1972; Roy et al., 1989; Brader et al., 1990, 1991). As the T_6–R_6 conversion proceeds to equilibrium (Figures 1–3), the spectrum of the intermediate is replaced by the spectrum of the distorted tetrahedral Co(II)–R_6 complex derived from the dominant ligand present in solution: herein, either phenoxide ion or, when present, chloride ion, thiocyanate ion, or iodide ion (Brader et al., 1990, 1991). The total change in absorbance (when phenoxide ion, chloride ion, or iodide ion is the coordinating ligand in the product) is approximately 10 times the absorbance maximum of the intermediate peak at 560 nm (Figures 1 and 2). When 5 mM thiocyanate ion is present, only a trace of the intermediate is detected (Figure 3). No intermediate was detected at higher thiocyanate ion concentrations, and none was detected in the azide ion system. The rate of appearance of the final spectrum closely coincides with the rate of decay of the intermediate. Although the spectrum of the final complex is strongly dependent on the nature of the anion coordinated to the fourth position, the spectrum of the intermediate does not depend on the nature of the anion present in solution. Hence, the intermediates detected by RSSF spectroscopy for the phenoxide, chloride, iodide, and thiocyanate systems all appear to exhibit the same spectrum even though the final spectra are quite different. Therefore, we conclude that the structure of the intermediate contains an exchangeable ligand derived from the initial Co(II)–T_6 complex rather than from the ligand coordinated to the fourth position of the Co(II)–R_6 product.

The results obtained for the scaled subtractions of the T_6–R_6 transition when thiocyanate ion or azide ion is present are interesting. The explanation seems straightforward: We postulate (Scheme I) that the intermediate is less prominent when 5 mM SCN^- is present, and absent at high SCN^- concentration, because SCN^- becomes coordinated to the metal center in the Co(II)–T_6 state in a rapid, preequilibrium process. Therefore, when phenol is added, successive RSSF spectra show only the buildup of a trace of the intermediate because most of the reaction proceeds directly from the Co(II)–T_6–thiocyanate complex to the Co(II)–R_6–thiocyanate complex. In the azide ion system, no intermediate is detected because essentially all of the reaction proceeds from the Co(II)–T_6–azide complex to the Co(II)–R_6–azide complex.

The equilibria shown in Scheme I describe the difference in mechanistic pathways between strong ligands, which give little or no intermediate in the T_6–R_6 transformation (counterclockwise path), and the relatively weak ligands, which give detectable amounts of the intermediate (clockwise path). When chloride, iodide, or phenoxide ions are present, we postulate that phenol first induces the T_6 or R_6 conformation change via binding to the protein pockets of the R-state, forming a water or hydroxide tetrahedral complex (steps designated L_0 and K_R^P). This transient intermediate then is

transformed to the final product by a slower, ligand-substitution process.

According to this hypothesis, the intermediate is a Co(II)–R-state species with at least one tetrahedral metal center wherein the fourth coordination site is occupied by either a water molecule or hydroxide ion. Prior to the addition of phenol, the preexisting distribution of states (step L_0) so strongly favors Co(II)–T_6 (the T_0-state) that the presence of the R-state is undetected in the UV–visible absorption profile. As shown in Scheme I, upon mixing with phenol, this distribution is shifted (in a rapid, preequilibrium step, K_R^P) as a consequence of the stabilization of the R-state by the binding of phenol to the protein pockets of the R_0-state. Through the positive cooperative heterotropic interactions resulting from the exchange of more stabilizing anions (designated X^- in Scheme I) such as phenoxide ion, Cl^-, or I^- into the fourth coordination site (Brader et al., 1991), the R-state is further stabilized and the overall distribution of species shifts in step $K_R^{P,X}$ to the anion-coordinated Co(II)–R_6 product species at a rate which probably is limited by the process which limits the rate of ligand exchange.[3] The spectrum of the intermediate is independent of pH over the pH range 7.0–9.5 (data not shown). Therefore, if the assignment of the structure of the intermediate to the tetrahedral R-state H_2O or OH^- complex is correct, then the value of $pK_a^{R,P}$ must be either less than ~6.5 or greater than ~10.

When strong anions such as thiocyanate or N_3^- are present, the rapid, ligand-substitution preequilibrium step designated K_T^X in Scheme I sufficiently favors the coordination of SCN^- such that the SCN^- or N_3^- coordinated Co(II)–T_6 species [the T_0(X)-state], when mixed with phenol, proceeds directly to the Co(II)–R_6–SCN^- or –N_3^- tetrahedral complex via the R_0(X)-state, and little or no detectable intermediate accumulates.[3] Scheme I is purposely written so that no attempt is made to distinguish between $T_6 \rightleftharpoons T_3R_3 \rightleftharpoons T_6$ and $T_6 \rightleftharpoons R_6$ allosteric transitions.[4] Crystallographic (Smith et al., 1984; Bentley et al., 1976; DeGraaff et al., 1981) and solution studies (Renscheidt et al., 1984; Wollmer et al., 1987; Kaarsholm et al., 1989; Brader et al., 1991) indicate that T_3R_3 may be a significant species on the pathway for the interconversion of T_6 and R_6.

Alternatively, the sequence depicted in Scheme I could be modified to yield a five-coordinate intermediate in which the metal sites are coordinated by three HisB10 imidazolyl moieties and two water molecules (or one water molecule and one hydroxide ion). According to this variation, substitution of a coordinated water molecule by the stabilizing anion and elimination of the remaining water (or hydroxide ion) drives the conversion of the intermediate to the anion-coordinated Co(II)–R_6 species. However, this variation can only explain the absence of a detectable intermediate in the N_3^- and SCN^- systems by postulating that the intermediate does not accumulate because decay is faster than intermediate formation. The available evidence does not provide a basis for distinguishing between a tetrahedral and a pentacoordinate geometry for the intermediate. Brader et al. (1991) have presented evidence indicating that although the Co(II)–R_6 species has a strong preference for tetrahedral coordination, certain ligands capable of bidentate ligation give five-coordinate complexes. Pyridine-2-thiol is the most unambiguous example; on the basis of the magnitudes of extinction coefficients and band positions, it is likely that acetate ion, nitrate ion, and bicarbonate ion also are coordinated in a bidentate fashion, giving five-coordinate complexes with Co(II)–R_6. While we are unable to distinguish between tetrahedral and pentacoordinate structures for the metal center of the intermediate, it is clear that an octahedral ligand field can be rejected. The *d–d* transitions which characterize the intermediate have intensities and band shapes that are inconsistent with assignment to an octahedral complex.

If the intermediate is properly identified as an R-state species, then these kinetic studies establish that the T to R allosteric transition[2] is a moderately rapid process. Nevertheless, this coil-to-helix transition is at least 6 orders of magnitude slower than the rate expected for the coil-to-helix transition of a simple peptide in solution. Previous work from this laboratory (Roy et al., 1989; Brader et al., 1990, 1991; Brader & Dunn, 1990) has established that, in addition to the Zn(II)- and Co(II)-substituted hexamers, the metal-free tetramer (Kadima, Lee, Kaarsholm, and Dunn, manuscript in preparation), the metal-free hexamer (Roy et al., 1989), and the Cu(II)- and Cu(I)-substituted hexamers (Brader & Dunn, 1990) all are capable of undergoing the T to R conformational transition. Comparisons of static spectra and substitutions of chemical probes indicate that the thermodynamics and kinetics of the transition depend upon the nature of the metal ion, the structure of the phenolic compound, and the nature of the fourth ligand (Roy et al., 1989; Brader et al., 1990, 1991; Brader & Dunn, 1990). These findings indicate that the allosteric transition is affected by ligand interactions at several loci and that both homotropic and heterotropic interactions play important roles in modulating the energetics of the transition.

[3] Comparison of reaction time courses for the phenol-induced transformation under the conditions described in Figures 1A,C and 3 in the absence and presence of 5 mM SCN^- established that the appearance of the final product occurs more rapidly when 5 mM SCN^- is present and that the rate of appearance is comparable to (but slightly slower than) the rate at which intermediate appears in the absence of SCN^- (data not shown). While we as yet have no independent means for measuring the rates at which phenolate ion, chloride ion, or azide ion substitute for a coordinated hydroxide ion (or a coordinated water molecule), our kinetic studies of ligand substitution reactions with the Co(II)–R_6–phenolate or –chloride complexes establish that ligand exchange occurs at rates which are consistent with the observed rates of intermediate decay (DeConinck and Dunn, unpublished results). Consequently, the rate behavior of these systems is consistent with Scheme I.

[4] Solutions of 1–2 mM pig zinc–insulin are reported to give crystals of T_3R_3 in the presence of either 0.30 M NaCl or 0.03 M KSCN. Our studies (Roy et al., 1989) indicate that substitution of Co(II) for Zn(II) renders the phenol-induced T to R transition of the human insulin hexamer less favorable by a factor of about 3. We have found that in the absence of phenol, the Co(II)-substituted hexamer shows no changes in the *d–d* transitions indicative of the formation of R-state species containing a tetrahedral metal center when 1 M NaCl is present (Roy et al., 1989; Brader et al., 1991; Choi, Brader, Aguilar, Kaarsholm, and Dunn, manuscript in preparation). In the presence of 5 mM SCN^-, only a trace of R-state is produced [see Figure 3 of Brader et al. (1991)]. It is unclear whether or not the SCN^--induced transition yields significant amounts of Co(II)–T_3R_3 in solution. In any event, the *d–d* envelope of the Co(II) species induced by SCN^- alone has a spectrum which is essentially identical to that of the Co(II)–R_6–thiocyanate adduct (Brader et al., 1991). Consequently, it seems unlikely that the intermediate detected in these transient kinetic experiments is simply due to Co(II)–T_3R_3.

ACKNOWLEDGMENTS

We thank Mark L. Brader, Eddie Choi, and Peter Brzovič for helpful and stimulating discussions, and we thank Peter Brzovič for technical assistance with the rapid-scanning stopped-flow studies.

Registry No. Insulin, 9004-10-8.

REFERENCES

Baker, E. N., Blundell, T. L., Cutfield, J. F., Cutfield, S. M., Dodson, E. J., Dodson, G. G., Hodgkin, D. C., Hubbard,

R. E., Isaacs, N. W., Reynolds, C. D., Sakabe, K., Sakabe, N., & Vijayan, N. M. (1988) *Philos. Trans. R. Soc. London, B 319*, 369-456.
Bentley, G. A., Dodson, E. J., Dodson, G. G., Hodgkin D. C., & Mercola, D. A. (1976) *Nature 261*, 166-168.
Brader, M. L., & Dunn, M. F. (1990) *J. Am. Chem. Soc. 112*, 4585-4587.
Brader, M. L., Kaarsholm, N. C., & Dunn, M. F. (1990) *J. Biol. Chem. 265*, 15666-15670.
Brader, M. L., Kaarsholm, N. C., Lee, R. W.-K., & Dunn, M. F. (1991) *Biochemistry 30*, 6636-6645.
Bunnett, J. F. (1974) *Techniques of Chemistry*, Vol. 4, Part I, pp 390-395, Wiley Interscience, New York.
Cotton, F. A., & Wilkinson, G. (1972) in *Advanced Inorganic Chemistry*, 3rd ed., p 885, Wiley Interscience, New York.
De Graaff, R. A. G., Lewit-Bentley, A., & Tolley, S. P. (1981) in *Structural Studies on Molecules of Biological Interest* (Dodson, G., Glusker, J. P., & Sayre, D., Eds.) pp 547-556, Clarendon Press, Oxford.
Derewenda, U., Derewenda, Z., Dodson, E. J., Dodson, G. G., Reynolds, C. G., Smith, G. D., Sparks, C., & Swensen, D. (1989) *Nature 338*, 594-596.
Kaarsholm, N. C., Ko, H.-C., & Dunn, M. F. (1989) *Biochemistry 28*, 4427-4435.
Koerber, S. C., MacGibbon, A. K. H., Dietrich, H., Zeppezauer, M., & Dunn, M. F. (1983) *Biochemistry 22*, 3424-3431.
Porter, R. R. (1953) *Biochem. J. 53*, 320-328.
Reinscheidt, H., Strassburger, W., Glatter, U., Wollmer, A., Dodson, G. G., & Mercola, D. A. (1984) *Eur. J. Biochem. 142*, 7-14.
Roy, M., Brader, M. L., Lee, R. W.-K., Kaarsholm, N. C., Hansen, J. F., & Dunn, M. F. (1989) *J. Biol. Chem. 264*, 19081-19085.
Smith, G. D., Swenson, D. C., Dodson, E. J., Dodson, G. G., & Reynolds, C. D. (1984) *Proc. Natl. Acad. Sci. U.S.A. 81*, 7093-7097.
Wollmer, A., Rannefeld, B., Johansen, B. R., Hejnaes, K. R., Blaschmidt, P., & Hansen, F. B. (1987) *Biol. Chem. Hoppe-Seyler 368*, 903-912.

Fluorescence, CD, Attenuated Total Reflectance (ATR) FTIR, and ^{13}C NMR Characterization of the Structure and Dynamics of Synthetic Melittin and Melittin Analogues in Lipid Environments†

Arthur J. Weaver,‡,§ Marvin D. Kemple,*,‖ Joseph W. Brauner,⊥ Richard Mendelsohn,⊥ and Franklyn G. Prendergast*,‡

Department of Biochemistry and Molecular Biology, Mayo Foundation, Rochester, Minnesota 55905, Department of Physics, Indiana University-Purdue University at Indianapolis, Indianapolis, Indiana 46205-2810, and Department of Chemistry, Rutgers University, Newark, New Jersey 07102

Received September 16, 1991

ABSTRACT: The structure and dynamics of synthetic melittin (MLT) and MLT analogues bound to monomyristoylphosphatidylcholine micelles, dimyristoylphosphatidylcholine vesicles, and diacylphosphatidylcholine films have been investigated by fluorescence, CD, attenuated total reflectance (ATR) FTIR, and ^{13}C NMR spectroscopy. All of these methods provide information about peptide secondary structure and/or about the environment of the single tryptophan side chain in these lipid environments. ATR-FTIR data provide additional information about the orientation of helical peptide segments with respect to the bilayer plane. Steady-state fluorescence anisotropy, fluorescence lifetime, and ^{13}C NMR relaxation data are used in concert to provide quantitative information about the dynamics of a single ^{13}C-labeled tryptophan side chain at position 19 in lipid-bound MLT, and at positions 17, 11, and 9, respectively, in lipid-bound MLT analogues. Peptide chain dynamics are probed by NMR relaxation studies of $^{13}C\alpha$-labeled glycine incorporated into each of the MLT peptides at position 12. The cumulative structural and dynamic data are consistent with a model wherein the N-terminal α-helical segment of these peptides is oriented perpendicular to the bilayer plane. Correlation times for the lysolipid-peptide complexes provide evidence for binding of a single peptide monomer per micelle. A model for the membranolytic action of MLT and MLT-like peptides is proposed.

Although the cytolytic action of the bee venom peptide melittin (MLT)[1] has long been recognized (Sessa et al., 1969), the biophysical mechanisms underlying its membranolytic effects are still unclear. Three fundamentally distinct hypotheses have been proposed. One asserts a perturbation of the membrane bilayer in which the peptide acts as a sort of mechanical "wedge" between lipid molecules, resulting in

† This work was supported in part by PHS Grant GM34847 to F.G.P. and GM29864 to R.M.

* Address correspondence to these authors.
‡ Mayo Foundation.
§ Current address: Howard Hughes Medical Institute, University of Texas Southwestern Medical Center, Dallas, TX 75235-9050.
‖ Indiana University-Purdue University at Indianapolis (IUPUI).
⊥ Rutgers University.

[1] Abbreviations: ATF-FTIR, attenuated total reflectance-Fourier transform infrared; CD, circular dichroism; CMC, critical micelle concentration; CPMG, Carr-Purcell-Meiboom-Gill; CSA, chemical shift anisotropy; DMPC, dimyristoyl-L-α-phosphatidylcholine; LDAO, lauryldimethylamineoxide; MLPC, monolauroyl-L-α-phosphatidylcholine; MLT, melittin; MLT-W19, ([$^{13}C\delta_1$]L-Trp19,[$^{13}C\alpha$]Gly12)melittin; MLT-W17, ([$^{13}C\delta_1$]L-Trp17,[$^{13}C\alpha$]Gly12,Leu19)melittin; MLT-W11, ([$^{13}C\delta_1$]L-Trp11,[$^{13}C\alpha$]Gly12,Leu19)melittin; MLT-W9, ([$^{13}C\delta_1$]L-Trp9,[$^{13}C\alpha$]Gly12,Leu19)melittin; MMPC, monomyristoyl-L-α-phosphatidycholine; NMR, nuclear magnetic resonance; NOE, nuclear Overhauser effect; POPC, palmitoyloleoyl-L-α-phosphatidylcholine; Tris, tris(hydroxymethyl)aminomethane.

0006-2960/92/0431-1301$03.00/0